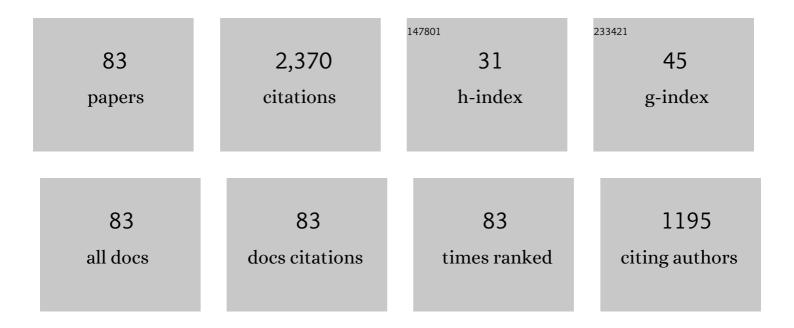
Xinzhao Chu

List of Publications by Year in descending order

Source: https://exaly.com/author-pdf/549031/publications.pdf Version: 2024-02-01



#	Article	IF	CITATIONS
1	NRLMSIS 2.0: A Wholeâ€Atmosphere Empirical Model of Temperature and Neutral Species Densities. Earth and Space Science, 2021, 8, e2020EA001321.	2.6	145
2	The Excitation of Secondary Gravity Waves From Local Body Forces: Theory and Observation. Journal of Geophysical Research D: Atmospheres, 2018, 123, 9296-9325.	3.3	85
3	Lidar observations of neutral Fe layers and fast gravity waves in the thermosphere (110-155 km) at McMurdo (77.8°S, 166.7°E), Antarctica. Geophysical Research Letters, 2011, 38, n/a-n/a.	4.0	84
4	Fe Boltzmann temperature lidar: design, error analysis, and initial results at the North and South Poles. Applied Optics, 2002, 41, 4400.	2.1	77
5	Lidar studies of interannual, seasonal, and diurnal variations of polar mesospheric clouds at the South Pole. Journal of Geophysical Research, 2003, 108, .	3.3	69
6	Seasonal variations of the Na and Fe layers at the South Pole and their implications for the chemistry and general circulation of the polar mesosphere. Journal of Geophysical Research, 2005, 110, .	3.3	69
7	Removal of Meteoric Iron on Polar Mesospheric Clouds. Science, 2004, 304, 426-428.	12.6	67
8	Gravity wave variations during the 2009 stratospheric sudden warming as revealed by ECMWFâ€₹799 and observations. Geophysical Research Letters, 2010, 37, .	4.0	62
9	Comparison of meteor radar and Na Doppler lidar measurements of winds in the mesopause region above Maui, Hawaii. Journal of Geophysical Research, 2005, 110, .	3.3	59
10	Inertiaâ€gravity waves in Antarctica: A case study using simultaneous lidar and radar measurements at McMurdo/Scott Base (77.8°S, 166.7°E). Journal of Geophysical Research D: Atmospheres, 2013, 118, 2794-2808.	3.3	58
11	Lidar observations of persistent gravity waves with periods of 3–10 h in the Antarctic middle and upper atmosphere at McMurdo (77.83°S, 166.67ŰE). Journal of Geophysical Research: Space Physics, 2016, 121, 1483-1502.	2.4	57
12	Stratospheric gravity wave characteristics and seasonal variations observed by lidar at the South Pole and Rothera, Antarctica. Journal of Geophysical Research, 2009, 114, .	3.3	55
13	First lidar observations of middle atmosphere temperatures, Fe densities, and polar mesospheric clouds over the north and south poles. Geophysical Research Letters, 2001, 28, 1199-1202.	4.0	52
14	Polar mesospheric clouds observed by an iron Boltzmann lidar at Rothera (67.5ŰS, 68.0ŰW), Antarctica from 2002 to 2005: Properties and implications. Journal of Geophysical Research, 2006, 111, .	3.3	48
15	Lidar observations of stratospheric gravity waves from 2011 to 2015 at McMurdo (77.84°S, 166.69°E), Antarctica: 1. Vertical wavelengths, periods, and frequency and vertical wave number spectra. Journal of Geophysical Research D: Atmospheres, 2017, 122, 5041-5062.	3.3	48
16	Antarctic mesospheric clouds formed from space shuttle exhaust. Geophysical Research Letters, 2005, 32, .	4.0	46
17	Resonance Fluorescence Lidar for Measurements of the Middle and Upper Atmosphere. Optical Science and Engineering, 2005, , 179-432.	0.1	46
18	Comparison of simultaneous Na lidar and mesospheric nightglow temperature measurements and the effects of tides on the emission layer heights. Journal of Geophysical Research, 2005, 110, .	3.3	45

Хілгнао Сни

#	Article	IF	CITATIONS
19	Vertical evolution of potential energy density and vertical wave number spectrum of Antarctic gravity waves from 35 to 105 km at McMurdo (77.8°S, 166.7°E). Journal of Geophysical Research D: Atmospheres, 2015, 120, 2719-2737.	3.3	41
20	Lidar observations of elevated temperatures in bright chemiluminescent meteor trails during the 1998 Leonid Shower. Geophysical Research Letters, 2000, 27, 1815-1818.	4.0	40
21	Responses of mesosphere and lower thermosphere temperatures to gravity wave forcing during stratospheric sudden warming. Geophysical Research Letters, 2010, 37, .	4.0	39
22	Observation of a thermospheric descending layer of neutral K over Arecibo. Journal of Atmospheric and Solar-Terrestrial Physics, 2013, 104, 253-259.	1.6	39
23	Validation of SABER v2.0 Operational Temperature Data With Groundâ€Based Lidars in the Mesosphere‣ower Thermosphere Region (75–105Âkm). Journal of Geophysical Research D: Atmospheres, 2018, 123, 9916-9934.	3.3	39
24	Lidar observations of thermospheric Na layers up to 170 km with a descending tidal phase at Lijiang (26.7°N, 100.0°E), China. Journal of Geophysical Research: Space Physics, 2015, 120, 9213-9220.	2.4	38
25	First observations of long-lived meteor trains with resonance lidar and other optical instruments. Geophysical Research Letters, 2000, 27, 1811-1814.	4.0	37
26	Nocturnal temperature structure in the mesopause region over the Arecibo Observatory (18.35°N,) Tj ETQq0 0	0 rggT /Ov	erlock 10 Tf
27	Lidar observations of polar mesospheric clouds at South Pole: Diurnal variations. Geophysical Research Letters, 2001, 28, 1937-1940.	4.0	36
28	Na double-edge magneto-optic filter for Na lidar profiling of wind and temperature in the lower atmosphere. Optics Letters, 2009, 34, 199.	3.3	36
29	Two-dimensional Morlet wavelet transform and its application to wave recognition methodology of automatically extracting two-dimensional wave packets from lidar observations in Antarctica. Journal of Atmospheric and Solar-Terrestrial Physics, 2017, 162, 28-47.	1.6	34
30	Formation mechanisms of neutral Fe layers in the thermosphere at Antarctica studied with a thermosphereâ€ionosphere Fe/Fe ⁺ (TIFe) model. Journal of Geophysical Research: Space Physics, 2017, 122, 6812-6848.	2.4	34
31	Lidar Observations of Stratospheric Gravity Waves From 2011 to 2015 at McMurdo (77.84°S, 166.69°E), Antarctica: 2. Potential Energy Densities, Lognormal Distributions, and Seasonal Variations. Journal of Geophysical Research D: Atmospheres, 2018, 123, 7910-7934.	3.3	33
32	Nocturnal thermal structure of the mesosphere and lower thermosphere region at Maui, Hawaii (20.7°N), and Starfire Optical Range, New Mexico (35°N). Journal of Geophysical Research, 2005, 110, .	3.3	32
33	Characteristics of Fe ablation trails observed during the 1998 Leonid Meteor Shower. Geophysical Research Letters, 2000, 27, 1807-1810.	4.0	31
34	Measurements of the vertical fluxes of atomic Fe and Na at the mesopause: Implications for the velocity of cosmic dust entering the atmosphere. Geophysical Research Letters, 2015, 42, 169-175.	4.0	31
35	First lidar observations of polar mesospheric clouds and Fe temperatures at McMurdo (77.8°S,) Tj ETQq1 1 0.73	84314 rgB7 4.0	「 /Overlock
36	High-efficiency receiver architecture for resonance-fluorescence and Doppler lidars. Applied Optics, 2015, 54, 3173.	2.1	30

Хілгнао Сни

#	Article	IF	CITATIONS
37	A thermospheric Na layer event observed up to 140 km over Syowa Station (69.0°S, 39.6°E) in Antarctica. Geophysical Research Letters, 2015, 42, 3647-3653.	4.0	28
38	A coordinated study of 1 h mesoscale gravity waves propagating from Logan to Boulder with CRRL Na Doppler lidars and temperature mapper. Journal of Geophysical Research D: Atmospheres, 2015, 120, 10,006.	3.3	28
39	Zonalâ€mean global teleconnection from 15 to 110 km derived from SABER and WACCM. Journal of Geophysical Research, 2012, 117, .	3.3	27
40	Lidar observations of polar mesospheric clouds at Rothera, Antarctica (67.5°S, 68.0°W). Geophysical Research Letters, 2004, 31, .	4.0	26
41	Eastward propagating planetary waves with periods of 1–5 days in the winter Antarctic stratosphere as revealed by MERRA and lidar. Journal of Geophysical Research D: Atmospheres, 2013, 118, 9565-9578.	3.3	26
42	Observations of persistent Leonid meteor trails: 1. Advection of the "Diamond Ring― Journal of Geophysical Research, 2001, 106, 21517-21524.	3.3	25
43	Observations of persistent Leonid meteor trails: 2. Photometry and numerical modeling. Journal of Geophysical Research, 2001, 106, 21525-21541.	3.3	25
44	Seasonal variations of the mesospheric Fe layer at Rothera, Antarctica (67.5°S, 68.0°W). Journal of Geophysical Research, 2011, 116, .	3.3	25
45	Responses of polar mesospheric cloud brightness to stratospheric gravity waves at the South Pole and Rothera, Antarctica. Journal of Atmospheric and Solar-Terrestrial Physics, 2009, 71, 434-445.	1.6	24
46	Field demonstration of simultaneous wind and temperature measurements from 5to50 km with a Na double-edge magneto-optic filter in a multi-frequency Doppler lidar. Optics Letters, 2009, 34, 1552.	3.3	23
47	Role of gravity waves in the spatial and temporal variability of stratospheric temperature measured by COSMIC/FORMOSATâ€3 and Rayleigh lidar observations. Journal of Geophysical Research, 2010, 115, .	3.3	22
48	Winter temperature tides from 30 to 110 km at McMurdo (77.8°S, 166.7°E), Antarctica: Lidar observation and comparisons with WAM. Journal of Geophysical Research D: Atmospheres, 2014, 119, 2846-2863.	^s 3.3	21
49	A reconfigurable all-fiber polarization-diversity coherent Doppler lidar: principles and numerical simulations. Applied Optics, 2015, 54, 8999.	2.1	21
50	Lidar observations of polar mesospheric clouds at South Pole: Seasonal variations. Geophysical Research Letters, 2001, 28, 1203-1206.	4.0	20
51	Diurnal variations of the Fe layer in the mesosphere and lower thermosphere: Four season variability and solar effects on the layer bottomside at McMurdo (77.8°S, 166.7°E), Antarctica. Journal of Geophysical Research, 2012, 117, .	3.3	19
52	First Simultaneous Lidar Observations of Thermosphereâ€lonosphere Fe and Na (TIFe and TINa) Layers at McMurdo (77.84°S, 166.67°E), Antarctica With Concurrent Measurements of Aurora Activity, Enhanced Ionization Layers, and Converging Electric Field. Geophysical Research Letters, 2020, 47, e2020GL090181.	4.0	19
53	Statistical characterization of high-to-medium frequency mesoscale gravity waves by lidar-measured vertical winds and temperatures in the MLT. Journal of Atmospheric and Solar-Terrestrial Physics, 2017, 162, 3-15.	1.6	18
54	Longitude variations of the solar semidiurnal tides in the mesosphere and lower thermosphere at low latitudes observed from ground and space. Journal of Geophysical Research, 2009, 114, .	3.3	17

Хілгнао Сни

#	Article	IF	CITATIONS
55	Simultaneous, commonâ€volume lidar observations and theoretical studies of correlations among Fe/Na layers and temperatures in the mesosphere and lower thermosphere at Boulder Table Mountain (40°N, 105°W), Colorado. Journal of Geophysical Research D: Atmospheres, 2013, 118, 8748-8759.	3.3	15
56	First Observations of Shortâ€Period Eastward Propagating Planetary Waves From the Stratosphere to the Lower Thermosphere (110Âkm) in Winter Antarctica. Geophysical Research Letters, 2017, 44, 10,744.	4.0	14
57	lodine-filter-based mobile Doppler lidar to make continuous and full-azimuth-scanned wind measurements: data acquisition and analysis system, data retrieval methods, and error analysis. Applied Optics, 2010, 49, 6960.	2.1	13
58	Statistics of sporadic iron layers and relation to atmospheric dynamics. Journal of Atmospheric and Solar-Terrestrial Physics, 2006, 68, 102-113.	1.6	11
59	Midâ€Latitude Thermosphereâ€lonosphere Na (TINa) Layers Observed With Highâ€Sensitivity Na Doppler Lidar Over Boulder (40.13°N, 105.24°W). Geophysical Research Letters, 2021, 48, e2021GL093729.	4.0	11
60	From Antarctica Lidar Discoveries to Oasis Exploration. EPJ Web of Conferences, 2016, 119, 12001.	0.3	9
61	Importance of Regionalâ€6cale Auroral Precipitation and Electrical Field Variability to the Stormâ€Time Thermospheric Temperature Enhancement and Inversion Layer (TTEIL) in the Antarctic E Region. Journal of Geophysical Research: Space Physics, 2020, 125, e2020JA028224.	2.4	9
62	Observations of persistent Leonid meteor trails 3. The "Glowworm― Journal of Geophysical Research, 2002, 107, SIA 5-1-SIA 5-10.	3.3	8
63	Lidar and CTIPe model studies of the fast amplitude growth with altitude of the diurnal temperature "tides―in the Antarctic winter lower thermosphere and dependence on geomagnetic activity. Geophysical Research Letters, 2015, 42, 697-704.	4.0	8
64	Shifts of the 3D - 4P transitions in different isotopes of positive calcium ions. Journal of Physics B: Atomic, Molecular and Optical Physics, 1997, 30, L677-L681.	1.5	7
65	Quasiâ€Biennial Oscillation of Shortâ€Period Planetary Waves and Polar Night Jet in Winter Antarctica Observed in SABER and MERRAâ€⊋ and Mechanism Study With a Quasiâ€Geostrophic Model. Geophysical Research Letters, 2019, 46, 13526-13534.	4.0	7
66	Eliminating photon noise biases in the computation of second-order statistics of lidar temperature, wind, and species measurements. Applied Optics, 2020, 59, 8259.	1.8	7
67	High frequency atmospheric gravity-wave properties using Fe-lidar and OH-imager observations. Geophysical Research Letters, 2005, 32, .	4.0	6
68	Investigation of a field-widened Mach–Zehnder receiver to extend Fe Doppler lidar wind measurements from the thermosphere to the ground. Applied Optics, 2016, 55, 1366.	2.1	6
69	First Lidar Observations of Quasiâ€Biennial Oscillationâ€Induced Interannual Variations of Gravity Wave Potential Energy Density at McMurdo via a Modulation of the Antarctic Polar Vortex. Journal of Geophysical Research D: Atmospheres, 2020, 125, e2020JD032866.	3.3	6
70	Dynamic Drivers of TIFe Diurnal Cycle in Antarctica. EPJ Web of Conferences, 2020, 237, 04002.	0.3	2
71	Comparison of Three Methodologies for Removal of Randomâ€Noiseâ€Induced Biases From Secondâ€Order Statistical Parameters of Lidar and Radar Measurements. Earth and Space Science, 2022, 9, .	2.6	2
72	Vertical Transport of Sensible Heat and Meteoric Na by the Complete Temporal Spectrum of Gravity Waves in the MLT Above McMurdo (77.84ËšS, 166.67ËšE), Antarctica. Journal of Geophysical Research D: Atmospheres, 0, , .	3.3	2

Χινζήλο Chu

#	Article	IF	CITATIONS
73	High spectral resolution test and calibration of an ultra-narrowband Faraday anomalous dispersion optical filter for use in daytime mesospheric resonance Doppler lidar. Journal of Atmospheric and Solar-Terrestrial Physics, 2012, 80, 187-194.	1.6	1
74	Antarctic Wave Dynamics Mystery Discovered by Lidar, Radar and Imager. EPJ Web of Conferences, 2016, 119, 13004.	0.3	1
75	Exploration of Whole Atmosphere Lidar: Mach-zehnder Receiver to Extend Fe Doppler Lidar Wind Measurements from the Thermosphere to the Ground. EPJ Web of Conferences, 2016, 119, 12004.	0.3	1
76	Winter Temperature and Tidal Structures from 2011 to 2014 at McMurdo Station: Observations from Fe Boltzmann Temperature and Rayleigh Lidar. EPJ Web of Conferences, 2016, 119, 12003.	0.3	1
77	Pole-to-pole: lidar observations of middle and upper atmosphere temperature and polar mesospheric clouds over the North and South Poles. , 2003, , .		0
78	Annual mesospheric midnight winds observed with a lidar at Starfire Optical Range, New Mexico. , 2003, 4893, 245.		0
79	Polar mesospheric clouds at the South Pole. , 2003, 4893, 504.		0
80	Simulation of Echoâ€Photon Counts of a Sodium Doppler Lidar and Retrievals of Atmospheric Parameters. Chinese Journal of Geophysics, 2010, 53, 519-528.	0.2	0
81	Low-latitude thermal semidiurnal tide: longitudinal and seasonal variations based on ground-based measurements from Arecibo and Maui, space-based measurements by SABER, and modeling with GSWM-02. , 2010, , .		0
82	Empirical Determination of Optimal Parameters for Sodium Double-Edge Magneto-Optic Filters. EPJ Web of Conferences, 2016, 119, 17012.	0.3	0
83	Simultaneous Observations of Mesoscale Gravity Waves Over the Central US with CRRL Na Doppler Lidars and USU Temperature Mapper. EPJ Web of Conferences, 2016, 119, 13003.	0.3	Ο